Journal of Experimental Nanoscience
Publication details, including instructions for authors and subscription information:
http://www.informaworld.com/smpp/title~content=t716100757

Fabrication and application of MFe_2O_4 (M = Zn, Cu) nanoparticles as anodes for Li ion batteries

Hongxiao Zhao[a]; Huimin Jia[a]; Shumin Wang[a]; Dengqi Xue[a]; Zhi Zheng[a]
[a] Institute of Surface Micro- and Nano-materials, Xuchang University, Xuchang, Henan 461000, P.R. China

Online publication date: 31 January 2011

To cite this Article Zhao, Hongxiao , Jia, Huimin , Wang, Shumin , Xue, Dengqi and Zheng, Zhi(2011) 'Fabrication and application of MFe_2O_4 (M = Zn, Cu) nanoparticles as anodes for Li ion batteries', Journal of Experimental Nanoscience, 6: 1, 75 — 83
To link to this Article: DOI: 10.1080/17458080.2010.487228
URL: http://dx.doi.org/10.1080/17458080.2010.487228

Journal of Experimental Nanoscience
Vol. 6, No. 1, February 2011, 75–83

Taylor & Francis
Taylor & Francis Group

Fabrication and application of MFe_2O_4 (M = Zn, Cu) nanoparticles as anodes for Li ion batteries

Hongxiao Zhao*, Huimin Jia, Shumin Wang, Dengqi Xue and Zhi Zheng*

Institute of Surface Micro- and Nano-materials, Xuchang University, Xuchang, Henan 461000, P.R. China

(*Received 30 December 2009; final version received 11 April 2010*)

In this work, MFe_2O_4 (M = Zn, Cu) nanoparticles were successfully prepared by a hydrothermal method. The structure, morphology, microstructure, specific surface area and electrochemical properties of the resultant particles were characterised by X-ray diffraction, scanning electron microscopy, transmission electron microscopy, nitrogen physical adsorption, charge–discharge test and cyclic voltammetry (CV) method, respectively. The resulting $ZnFe_2O_4$ and $CuFe_2O_4$ products were sphere-like and cubic-shaped particles and their average size was about 30–40 nm and 60–70 nm, respectively. The initial discharge capacities of $ZnFe_2O_4$ and $CuFe_2O_4$ electrodes reached 1287.5 mAh g^{-1} and 1412.3 mAh g^{-1}, respectively, at a current density of 0.2 mA cm^{-2} in a potential range of 0.0–3.0 V. This indicated that Cu is a better counter ion than Zn. The resulting MFe_2O_4 nanoparticles are expected to be a promising candidate of anode materials for Li ion batteries. The reaction mechanism of MFe_2O_4 nanoparticles in Li ion batteries was also discussed based on the CV of Li/MFe_2O_4 cell.

Keywords: MFe_2O_4 nanoparticles; Li ion batteries; electrochemical properties

1. Introduction

The increasing demand for rechargeable batteries for portable electronic devices and the need for high energy and power density batteries for electric vehicles and hybrid electric vehicles have generated a significant research interest in the electrode materials of Li ion batteries. In recent years, the electrochemical properties of the iron base compounds [1–4] with varied morphology and crystal structure have drawn much attention as an alternative for the traditional carbon materials anodes in Li ion batteries due to their relatively low cost and being environmental friendly. Among these materials, many ferrite materials [5,6] have exhibited better electrochemical properties than conventional materials used as anodes in Li ion batteries.

Most transition metal oxides (MO) can react with Fe_2O_3 to form ferrite MFe_2O_4 and the attractive feature of ferrite materials is that their properties especially magnetic, can be

*Corresponding authors. Email: zhaoxiao124@yahoo.com.cn; zhengzhi9999@yahoo.com.cn

ISSN 1745–8080 print/ISSN 1745–8099 online

DOI: 10.1080/17458080.2010.487228
http://www.informaworld.com

controlled in a broad measure to suit the particular application. Therefore, transition metal ferrite materials [7–10] have been widely studied as magnetic materials and many different fabrication methods such as sol–gel route [11,12], co-precipitation [13,14], hydrothermal method [15,16] and electrochemical method [17,18] have been applied. As a fabrication method, the hydrothermal process has characteristic features: it enables synthesis of materials at a far lower temperature [19], and the desired crystalline powders are directly prepared in the hydrothermal treatment. Furthermore, the need for high-temperature calcinations, and subsequent grinding processes are eliminated. The hydrothermal method has been used to prepare many ferrite materials [20–22] with outstanding magnetic properties. Being a transition metal, ferrite $ZnFe_2O_4$ has already been extensively investigated as magnetic material, but studies of its electrochemical properties in Li ion batteries are scarce, [5,23]. After Alcántara et al. [24] first proposed that $CuFe_2O_4$ could be used as anode in Li ion batteries, Kalai Selvan et al. [25] and NuLi and Qin [4] have studied the electrochemical behaviour of $CuFe_2O_4$. However, only a few discharge capacities of ferrite materials were reported by NuLi. In others reports, $ZnFe_2O_4$ and $CuFe_2O_4$ were all synthesised by the combustion method and thus the high temperature and long reaction time were necessary. In our previous work [26], the excellent electrochemical properties of $NiFe_2O_4$ nanoparticles have been demonstrated by taking advantage of the hydrothermal method. It is expected that the MFe_2O_4 nanoparticles with fine electrochemical properties could generally be prepared with this simple hydrothermal approach.

In this study, we attempt to continue our research on nanocrystalline metal ferrite particles used as anode materials for Li ion batteries and their electrochemical performance. $ZnFe_2O_4$ and $CuFe_2O_4$ nanoparticles were prepared by a mild hydrothermal method at a low temperature. The morphology, microstructure and special surface area (BET, Brunauer, Emmett and Teller) of the as-synthesised materials (MFe_2O_4) were investigated by X-ray diffraction (XRD), scanning electron microscopy (SEM), transmission electron microscopy (TEM) and nitrogen physical absorption. The electrochemical properties were also studied by charge–discharge test and cyclic voltammetry (CV).

2. Experimental procedure

2.1. *Synthesis of MFe_2O_4 nanoparticles*

The synthesis of MFe_2O_4 nanoparticles is similar to that described in literature [26] and described briefly as follows. All the chemical reagents used in the experiments were analytical reagent (AR) and without further purification. $Zn(CH_3OOH)_2 \cdot 2H_2O$, $Fe(NO_3)_3 \cdot 9H_2O$and Cu $(NO_3)_3 \cdot H_2O$ were used as precursors of MFe_2O_4 for the hydrothermal method. In a typical synthesis, the powders were mixed in the atomic ratio (M : Fe) of 1 : 2. The homogeneous solution was magnetically stirred for 2 h in air, and then the pH was adjusted with ammonia solution. Then the solution was transferred to a Teflon-lined stainless steel autoclave. The hydrothermal reaction was carried out at 230°C for 0.5 h and then cooled to room temperature. Finally, the MFe_2O_4 was obtained after the resulting precipitate was washed with distilled water several times and dried at 80°C.

2.2. *Characterisation of MFe_2O_4 nanoparticles*

Powder XRD patterns were obtained on a Rigaku powder diffractometer operating at 40 kV and 25 mA, using Cu-Kα radiation. Data were collected in the range from 20°C to 70°C in the 2θ-scale. Sample morphologies were examined in a FEI XL-30 SIRION SEM operating at 15 kV and in a Philips CM-120 TEM operating at 120 kV. The samples for TEM were prepared by dispersing the final powders in ethanol; the dispersion was then dropped on copper grids. Specific surface areas were measured by the BET method using N_2 gas as an adsorbent at liquid nitrogen temperature (Micromeritics Gemini 2380). The samples were dried at 80°C for 8 h and then degassed at 300°C for 2 h prior to the analysis of the surface areas.

2.3. *Electrochemical measurements*

The slurry consisting of an active material (synthesised material), a conducting agent (acetylene black) and a binder, polyvinylidene fluoride (PVDF) was smeared onto a copper foil, with *n*-methylpyrrolidone (NMP) as a solvent. The weight ratio of active material, conducting agent and binder was 85 : 10 : 5 in the working electrode. After being dried in air at 80°C for 4 h, the electrode was pressed and then dried at 120°C for 5 h in vacuum. Electrochemical tests were performed in two-electrode cell using metallic Li as both reference and counter electrodes. A solution of ethylene carbonate (EC) and diethyl carbonate (DEC) (1:1 volume ratio) with 1 mol $LiClO_4$ was used as an electrolyte. All cells were assembled in an Ar-filled glove box. The discharge–charge curves were tested galvanostatically at a current density of 0.2 mA cm^{-2} in a voltage window of 0.0–3.0 V versus Li^+/Li using computer controlled cycling equipment (BT2000 cell testing system, Arbin). Cyclic voltammogram (CV) was carried out in the potential range of 0.0–3.0 V versus Li^+/Li at a scan rate of 0.1 mv s^{-1}. All the tests were performed at room temperature.

3. Results and discussion

3.1. *XRD pattern*

The XRD patterns of as-prepared MFe_2O_4 (M = Zn, Cu) powders are shown in Figure 1. According to the JCPDS reference (1–1109) of $ZnFe_2O_4$ and (77–10) of $CuFe_2O_4$, the as-prepared powder materials were readily identified to be $ZnFe_2O_4$ (Figure 1(a)) and $CuFe_2O_4$ (Figure 1(b)), respectively. The Scherrer equation ($D = \kappa\lambda/\beta 1/2\cos\theta$) [27] was used to estimate the average sizes of the resulting MFe_2O_4 particles. The average crystallite sizes of MFe_2O_4 particles were calculated to be about 32 nm for $ZnFe_2O_4$ and 58 nm for $CuFe_2O_4$ taking coefficient κ to be 0.9.

3.2. *Morphologies of the resulting samples*

The morphology and microstructure of MFe_2O_4 nanoparticles was observed with SEM, as shown in Figure 2. SEM observation (Figure 2) reveals that the products were composed of a large number of particles. The morphologies and sizes of both $ZnFe_2O_4$ and $CuFe_2O_4$ nanoparticles were further characterised by transmission electron microscopy. The TEM

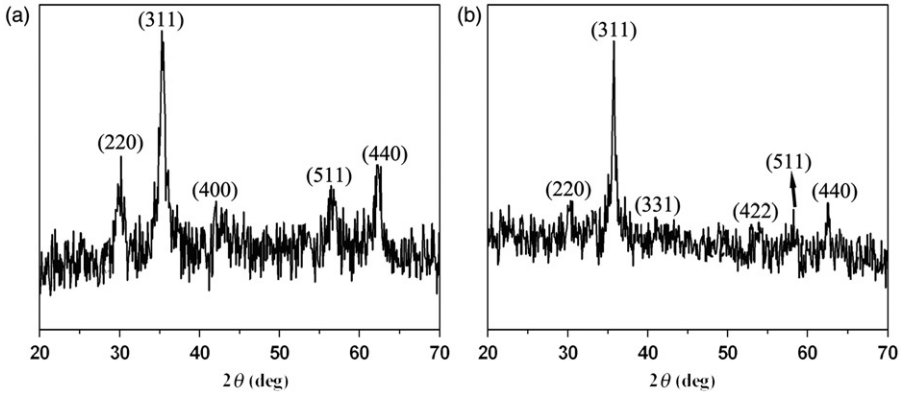

Figure 1. XRD reflections of resulting powders (a) $ZnFe_2O_4$ and (b) $CuFe_2O_4$.

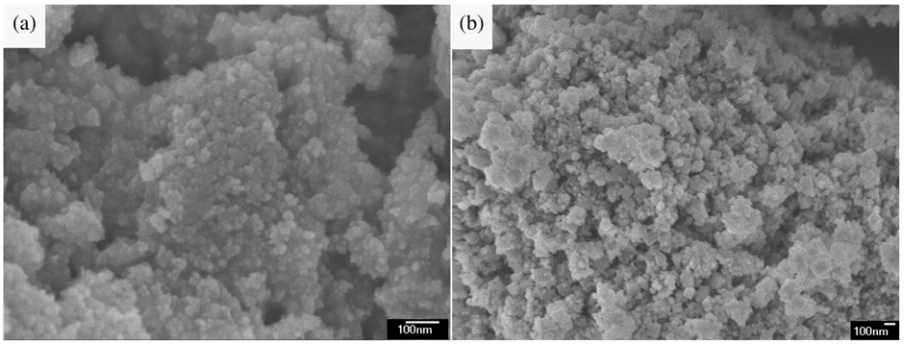

Figure 2. SEM images of the synthesised samples (a) $ZnFe_2O_4$ and (b) $CuFe_2O_4$.

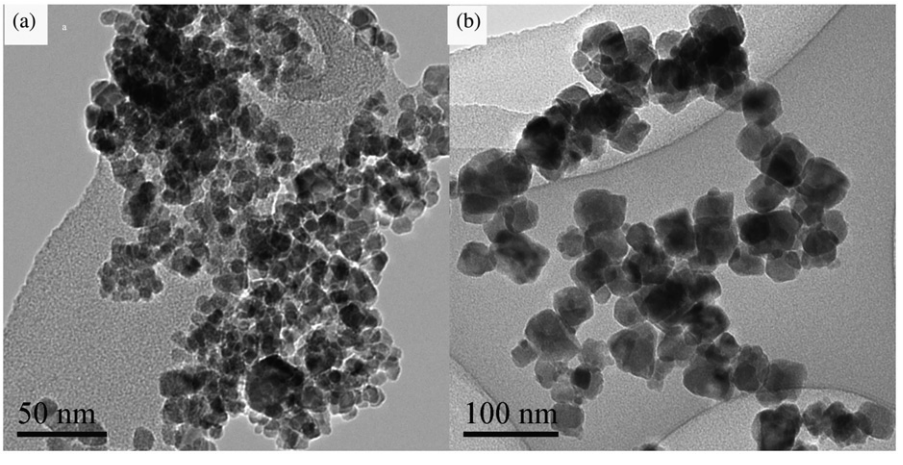

Figure 3. TEM morphologies of the obtained materials (a) $ZnFe_2O_4$ and (b) $CuFe_2O_4$.

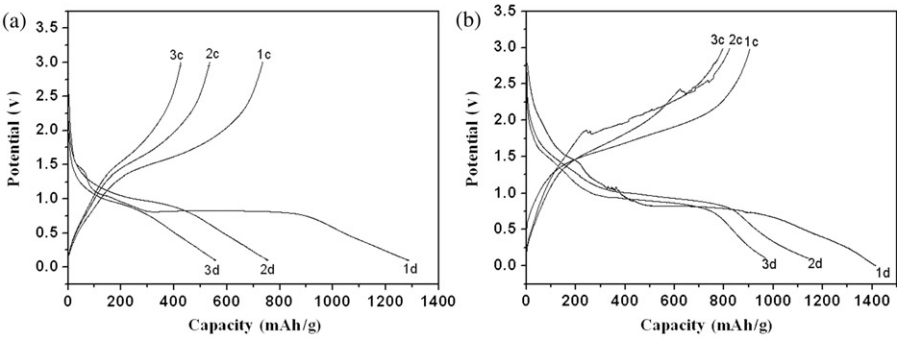

Figure 4. Charge–discharge curves of MFe_2O_4 nanoparticles (a) $ZnFe_2O_4$ and (b) $CuFe_2O_4$ during the first to third cycles at a voltage window of 3.0–0 V.

images (Figure 3) confirmed that the diameters of the as-synthesised irregular $ZnFe_2O_4$ were less than 30 nm, which was much smaller than that of the obtained cube-like $CuFe_2O_4$ nanoparticles. The average size of cube-like $CuFe_2O_4$ nanopartiles was estimated to be 60–70 nm. These results were well consistent with the XRD analysis.

3.3. *Electrochemical properties of the resulting MFe_2O_4 nanoparticles*

3.3.1. *Charge–discharge curves*

Figure 4 shows the first three cycles in discharge–charge curves of the MFe_2O_4 electrodes. From Figure 4, we can find that the MFe_2O_4 nanparticles exhibit an initial high-discharge capacity of 1287.5 mAh g^{-1} for $ZnFe_2O_4$ and 1412.3 mAh g^{-1} for $CuFe_2O_4$, respectively. The discharge capacity of the nanoparticles decayed to 746.0 mAh g^{-1} for $ZnFe_2O_4$ and 1143.3 mAh g^{-1} for $CuFe_2O_4$ in the second cycle, and became 560.3 mAh g^{-1} for $ZnFe_2O_4$ and 968.4 mAh g^{-1} for $CuFe_2O_4$ in the third cycle. Similar to the discharge capacity, the charge capacity also slightly decreased with the increase in the cycle numbers. The initial discharge capacity of $CuFe_2O_4$ obtained at low temperature was higher than that of the literature [28]. In the literature, Bomio et al. [28] reported that $CuFe_2O_4$ could retain a first discharge capacity of 1180 mAh g^{-1}. As can be seen, the first discharge-curve of $ZnFe_2O_4$ starts from the open circuit voltage (OCV $\sim$ 2.3 V) and shows a continuous decrease, through a single-phase Li-intercalation reaction, to reach a voltage plateaux region at $\sim$0.8 V.

It is interesting to note that the initial discharge capacity of $ZnFe_2O_4$ and $CuFe_2O_4$ is even higher than the theoretical value for a complete reduction from transition ions to the metallic state accompany with the formation of $8Li_2O$ per formula. The excess irreversible capacity may be related to the following two factors. One is the large surface area that is facilitated by the smaller particle size. Another is the irreversible reactions of MFe_2O_4 nanoparticles with electrolyte accompanied with the amorphisation of nanocrystalline MFe_2O_4, when the cell potential approaches to 0.0 V against Li^+/Li. Similar phenomena were also observed at the end of the discharge of $Li/CoFe_2O_4$ cells [29].

The BET surface area was further measured to explain the excellent electrochemical performance of the resulting MFe_2O_4 nanoparticles. As expected, the surface area of

$CuFe_2O_4$ and $ZnFe_2O_4$ is up to $98.4\,m^2\,g^{-1}$ and $99.5\,m^2\,g^{-1}$, respectively. These values are higher than those found in the literature [30,31]. Actually, the initial high discharge capacity of the MFe_2O_4 nanoparticles can be attributed to the large surface area and short diffusion distances provided by the nanostructures [32]. A large surface area leads to intimate contact between electrode material and electrolyte. It increases the actual reaction area and facilitates the transportation of Li ions [33]. The initial discharge capacity of $CuFe_2O_4$ is higher than that of $ZnFe_2O_4$, which is consistent with the relation of charge capacity. This was possibly caused by the influence of the surface area on the charge–discharge capacity.

3.3.2. *Cyclic voltammetry*

The CVs of $ZnFe_2O_4$ and $CuFe_2O_4$ powders for the first three cycles at a scan rate of $0.1\,mV\,s^{-1}$ in a potential range of 0.0–3.0 V are shown in Figure 5(a) and (b), respectively. For the $ZnFe_2O_4$ powder electrode, there is a substantial difference between the first and the subsequent cycles. The first cycle shows an irreversible reduction peak A with a maximum of about 2.0 V, which disappears in the subsequent cycles. Peaks B and C located at 1.4 and 0.6 V, respectively, appear in the first cycle and amalgamate into one broad peak. Peak A could be associated with the irreversible reaction for the reduction of the electrolyte [23]. Peaks B and C could be due to the reduction reaction of Fe^{3+} and Zn^{2+}. Peak B is the oxidation reactions of both metallic Fe and Cu. Combining this phenomenon and the fact that the charge–discharge curves are similar to the literature [5], it can be concluded that the reaction of Li with $ZnFe_2O_4$ is as follows:

$$ZnFe_2O_4 + 8Li^+ + 8e^- \rightarrow Zn + 2Fe + 4Li_2O$$

$$Zn + 2Fe + 3Li_2O \leftrightarrow LiZn + ZnO + 2FeO + 5Li^+ + 5e^-.$$

For the $CuFe_2O_4$ powder electrodes, a cathodic peak A located at around 0.85 V is probably associated with the reduction reaction of Fe^{3+} and Cu^{2+} with Li during the first cycle of $CuFe_2O_4$ electrodes. The two reduction peaks of Fe^{3+} and Cu^{2+} at 0.4 V could be overlapped to form the same peak (A) with high intensity under our experimental

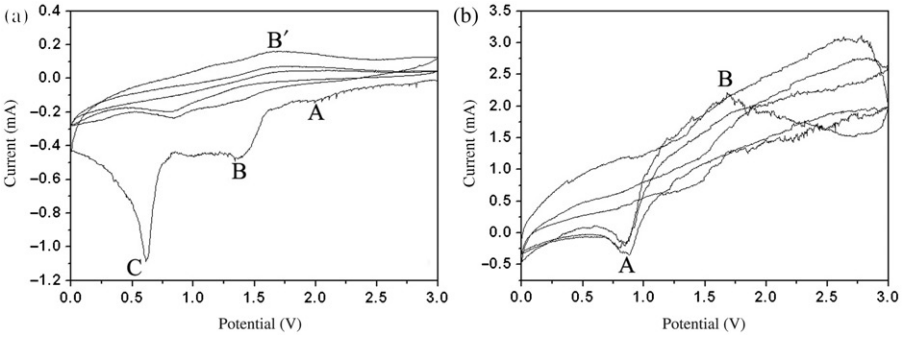

Figure 5. CV curves of (a) $ZnFe_2O_4$ and (b) $CuFe_2O_4$ (cycling conditions: in a potential range of 0.0–3.0 V, scan rate of $0.1\,mV\,s^{-1}$).

conditions. The anodic peak at around 1.7 V (B) is attributed to the oxidation reactions of both metallic Fe and Cu. Therefore, the reversible electrochemical reaction of Li with $CuFe_2O_4$ is a conversion reaction, similar to that of transition metal oxide anodes [3,4,34,35], which can be described by the following equation:

$$CuFe_2O_4 + 8Li^+ + 8e^- \rightarrow 4Li_2O + Cu + 2Fe$$

$$Cu + 2Fe + 4Li_2O \leftrightarrow CuO + Fe_2O_3 + 8Li^+ + 8e^-.$$

4. Conclusions

We described a general and efficient hydrothermal approach for synthesising MFe_2O_4 nanoparticles that can be potentially used as anodes for Li ion batteries. The resulting $ZnFe_2O_4$ and $CuFe_2O_4$ powders were spherical- and cubic-shaped particles and their average size was about 30–40 nm and 60–70 nm, respectively. Especially, $CuFe_2O_4$ nanoparticles with surface area of $98.4\,m^2\,g^{-1}$ exhibited better electrochemical properties with the higher initial discharge capacity of $1412.3\,mAh\,g^{-1}$ at a current density of $0.2\,mA\,cm^{-2}$ in a potential range of 0.0–3.0 V as anodes for Li ion batteries. From these results, $CuFe_2O_4$ nanoparticles were considered to be more suitable as a promising candidate of anode materials for Li ion batteries. Future research is currently in progress to optimise the anode composition and microstructure.

Acknowledgements

This work was supported by National Natural Science Foundation of China (grant no. 20873118), Program for New Century Excellent Talents in University (grant no. NCET-08-0665), the Programme for Science and Technology Innovation Talents in Universities of Henan Province (2008 HASTIT016), Henan Province Science and Technology Key Project (grant no. 082102230036) and Natural Science Foundation of Henan Province, China (grant nos 2008B150019 and 2009B150024).

References

[1] M. Hibino, J. Terashima, and T. Yao, *Reversible and rapid discharge–charge performance of γ-Fe_2O_3 prepared by aqueous solution method as the cathode for Lithium-ion battery*, J. Electrochem. Soc. 154 (2007), pp. A1107–A1111.

[2] E. Hosono, S. Fujihara, I. Honma, M. Ichihara, and H. Zhou, *Fabrication of nano/micro hierarchical Fe_2O_3/Ni micrometer-wire structure and characteristics for high rate Li rechargeable battery*, J. Electrochem. Soc. 153 (2006), pp. A1273–A1278.

[3] R. Alcántara, M. Jaraba, P. Lavela, J.L. Tirado, J.C. Jumas, and J. Olivier-Fourcade, *Changes in oxidation state and magnetic order of iron atoms during the electrochemical reaction of lithium with $NiFe_2O_4$*, Electrochem. Commun. 5 (2003), pp. 16–21.

[4] Y.N. NuLi and Q.Z. Qin, *Nanocrystalline transition metal ferrite thin films prepared by an electrochemical route for Li-ion batteries*, J. Power Sources 142 (2005), pp. 292–297.

[5] Y. Sharma, N. Sharma, G.V. Subba Rao, and B.V.R. Chowdari, *Li-storage and cyclability of urea combustion derived $ZnFe_2O_4$ as anode for Li-ion batteries*, Electrochim. Acta 53 (2008), pp. 2380–2385.

[6] X.D. Li, W.S. Yang, F. Li, D.G. Evans, and X. Duan, *Stoichiometric synthesis of pure $NiFe_2O_4$ spinel from layered double hydroxide precursors for use as the anode material in lithium-ion batteries*, J. Phys. Chem. Solids 67 (2006), pp. 1286–1290.
[7] C.D. Lokhande, S.S. Kulkarni, R.S. Mane, and S.H. Han, *Room temperature single-step electrosynthesized copper ferrite thin films and study of their magnetic properties*, J. Magn. Magn. Mater. 313 (2007), pp. 69–75.
[8] V. Berbenni, C. Milanese, G. Bruni, A. Marini, and I. Pallecchi, *Synthesis and magnetic properties of $ZnFe_2O_4$ obtained by mechanochemically assisted low-temperature annealing of mixtures of Zn and Fe oxalates*, Thermochim. Acta 447 (2006), pp. 184–189.
[9] H. Deng, H. Chen, and H. Li, *Synthesis of crystal MFe_2O_4 ($M = Mg$, Cu, Ni) microspheres*, Mater. Chem. Phys. 101 (2007), pp. 509–513.
[10] S. Maensiri, C. Masingboon, B. Boonchom, and S. Seraphin, *A simple route to synthesize nickel ferrite($NiFe_2O_4$) nanoparticles using egg white*, Scr. Mater. 56 (2007), pp. 797–800.
[11] H. Wang, F. Zhang, W. Zhang, X. Wang, Z. Lu, Z. Qian, Y. Sui, D. Dong, and W. Su, *The effect of surface modication on the morphology and magnetic properties of $NiFe_2O_4$ nanoparticles*, J. Cryst. Growth 293 (2006), pp. 169–174.
[12] S. Roy and J. Ghose, *Mössbauer study of nanocrystalline cubic $CuFe_2O_4$ synthesized by precipitation in polymer matrix*, J. Magn. Magn. Mater. 307 (2006), pp. 32–37.
[13] X.H. Yang, X. Wang, and Z.D. Zhang, *Electrochemical properties of submicron cobalt ferrite spinel through a co-precipitation method*, J. Cryst. Growth 277 (2005), pp. 467–470.
[14] M. Bonini, A. Wiedenmannb, and P. Baglioni, *Study of ferrite ferrofluids by small-angle scattering of polarized neutrons*, J. Appl. Crystallogr. 40 (2007), pp. s254–s258.
[15] L. Satyanarayana, K. Madhusudan Reddy, and S.V. Manorama, *Nanosized spinel $NiFe_2O_4$: A novel material for the detection of liquid petroleum gas in air*, Mater. Chem. Phys. 82 (2003), pp. 21–26.
[16] S.J. Stewart, S.J.A. Figueroa, M.B. Sturla, R.B. Scorzellic, F. García, and F.G. Requejo, *Magnetic $ZnFe_2O_4$ nano ferrites studied by X-ray magnetic circular dichroism and Mössbauer spectroscopy*, Physica B 389 (2007), pp. 155–158.
[17] D. Carlierz and J.P. Ansermet, *Electrochemical synthesis and magnetic properties of $CoFe_2O_4$ nanowire arrays*, J. Electrochem. Soc. 153 (2006), pp. C277–C281.
[18] M.K. Roy and H.C. Verma, *Magnetization anomalies of nanosize zinc ferrite particles prepared using electrodeposition*, J. Magn. Magn. Mater. 306 (2006), pp. 98–102.
[19] Y.Y. Liang, S.J. Bao, and H.L. Li, *A series of spinel phase cathode materials prepared by a simple hydrothermal process for rechargeable lithium batteries*, J. Solid State Chem. 179 (2006), pp. 2133–2140.
[20] M.M. Bucko and K. Haberko, *Hydrothermal synthesis of nickel ferrite powders, their properties and sintering*, J. Eur. Ceram. Soc. 27 (2007), pp. 723–727.
[21] X.X. Bo, G.S. Li, X.Q. Qiu, Y.F. Xue, and L.P. Li, *Magnetic diphase nanostructure of $ZnFe_2O_4$/γ-Fe_2O_3*, J. Solid State Chem. 180 (2007), pp. 1038–1044.
[22] C.Q. Hu, Z.H. Gao, and X.R. Yang, *One-pot low temperature synthesis of MFe_2O_4 ($M = Co$, Ni, Zn) superparamagnetic nanocrystals*, J. Magn. Magn. Mater. 320 (2008), pp. L70–L73.
[23] Y.N. NuLi, Y.Q. Chu, and Q.Z. Qin, *Nanocrystalline $ZnFe_2O_4$ and Ag-doped $ZnFe_2O_4$ films used as new anode materials for Li-ion batteries*, J. Electrochem. Soc. 151 (2004), pp. A1077–A1083.
[24] R. Alcántara, M. Jaraba, P. Lavela, and J.L. Tirado, Electrochemical lithium reaction of some first row transition-metal spinel mixed-oxides, Electrochemical society meeting, Salt Lake City, UT, 2002.
[25] R. Kalai Selvan, N. Kalaiselvi, C.O. Augustin, C.H. Doh, and C. Sanjeeviraja, *$CuFe_2O_4$/SnO_2 nanocomposites as anodes for Li-ion batteries*, J. Power Sources 157 (2006), pp. 522–527.

[26] H.X. Zhao, Z. Zheng, K.W. Wong, S.M. Wang, B.J. Huang, and D.P. Li, *Fabrication and electrochemical performance of nickel ferrite nanoparticles as anode material in lithium ion batteries*, Electrochem. Commun. 9 (2007), pp. 2606–2610.
[27] B.D. Cullity, *Elements of X-ray Diffraction*, Addison–Wesley Publishing Company, Reading, MA, 1956.
[28] M. Bomio, P. Lavela, and J.L. Tirado, *Electrochemical evaluation of $CuFe_2O_4$ samples obtained by sol–gel methods used as anodes in lithium batteries*, J. Solid State Electrochem. 12 (2008), pp. 729–737.
[29] Y.Q. Chu, Z.W. Fu, and Q.Z. Qin, *Cobalt ferrite thin films as anode material for lithium ion batteries*, Electrochim. Acta 49 (2004), pp. 4915–4921.
[30] M.B. Mona, B. Sarah, and P. Octavio, *Synthesis and characterization of $Zn_{1-x}Ni_xFe_2O_4$ spinels prepared by a citrate precursor*, J. Solid State Chem. 178 (2005), pp. 1080–1086.
[31] N.S. Chen, X.J. Yang, E.S. Liu, and J.L. Huang, *Reducing gas-sensing properties of ferrite compounds MFe_2O_4 ($M = Cu$, Zn, Cd and Mg)*, Sens. Actuat. B 66 (2000), pp. 178–180.
[32] Y. Wang, K. Takahashi, H.M. Shang, and G.Z. Cao, *Synthesis and Electrochemical properties of vanadium pentoxide nanotube arrays*, J. Phys. Chem. B 109 (2005), pp. 3085–3088.
[33] K. Takahashi, M. Saitoh, N. Asakura, T. Hibino, M. Sano, M. Fujita, and K. Kifune, *Electrochemical properties of lithium manganese oxides with different surface areas for lithium ion batteries*, J. Power Sources, 136 (2004), pp. 115–121.
[34] N. Sharma, K.M. Shaju, G.V. Subba Rao, and B.V.R. Chowdari, *Iron–tin oxides with $CaFe_2O_4$ structure as anodes for Li-ion batteries*, J. Power Sources 124 (2003), pp. 204–212.
[35] M. Bomio, P. Lavela, and J.L. Tirado, *^{57}Fe Mössbauer spectroscopy and electron microscopy study of metal extraction from $CuFe_2O_4$ electrodes in Lithium cells*, ChemPhysChem 8 (2007), pp. 1999–2007.